Coupled Electron-Proton Transfer in Interactions of Triplet C_{60} with Hydrogen-Bonded Phenols: Effects of Solvation, Deuteration, and Redox Potentials

László Biczók, Neeraj Gupta, and Henry Linschitz*

Contribution from the Department of Chemistry, Brandeis University, Waltham, Massachusetts 02254, and Central Research Institute for Chemistry, Hungarian Academy of Sciences, P.O. Box 17, 1525, Budapest, Hungary

Received August 7, 1997[⊗]

Abstract: The quenching of triplet C_{60} by phenols is greatly enhanced by addition of pyridines, which also lower the phenol voltammetric oxidation potentials. Flash photolysis shows that the products of this quenching reaction are the $C_{60}^{\bullet-}$ anion radical, neutral phenoxy (or naphthoxy) radicals, and protonated pyridines. Analysis of the second-order kinetics gives quenching rate constants and values of formation constants of hydrogen-bonded phenol−pyridine pairs. The latter agree with those derived from absorption spectra over a wide range of phenols, pyridines, and solvents. Significant deuterium kinetic isotope effects are observed, indicating the importance of both proton transfer and hydrogen bonding in enhancing the rate. Quenching rates and radical yields both increase with solvent polarity. It is concluded that this quenching process involves interaction between $^3C_{60}$ and a hydrogen-bonded phenol−pyridine complex, in which electron transfer from the phenol to $^3C_{60}$ is concerted with proton transfer from phenol to hydrogen-bonded pyridine.

Introduction

In connection with the general problem of coupled electron−proton transfer, we have recently given evidence for the occurrence of *concerted* charge movement to *different* acceptors, as exemplified in the pyridine-enhanced quenching by phenols or naphthols of triplet C_{60}[1,2] or tetracene fluorescence.[1] In the triplet C_{60} case, the actual quenching species was identified as the hydrogen-bonded phenol− or naphthol−pyridine pair, since formation equilibrium constants derived on this assumption from the second-order kinetics agreed with those obtained more directly from absorption spectra. Quenching of $^3C_{60}$ by the 2-naphthol−trimethylpyridine complex resulted in formation of $C_{60}^{\bullet-}$ anion and neutral naphthoxy radicals.[2] In addition, an appreciable deuterium isotope effect was found in quenching of tetracene fluorescence by phenol−pyridine systems.[1] It was therefore concluded that, in these interactions, electron transfer from the phenol moiety to the excited molecule is concerted with proton movement from the phenol −OH to the hydrogen-bonded base. The relation of such proton transfer to both the rate and free enthalpy change in the reaction was indicated.[1] These results on reductive quenching by phenols suggest analogies with the appearance of neutral tyrosine radicals in the electron transfer chain of Photosystem II in green plant photosynthesis.[3]

We now extend the C_{60} studies to a much wider range of phenols, pyridines, and other bases and solvents. We obtain additional comparisons between kinetically and spectroscopically determined H-bonding constants. To complete identification of all quenching reaction products, we demonstrate protonation of the hydrogen-bonded base (benzoquinoline), accompanying formation of $C_{60}^{\bullet-}$ and phenoxy radicals. Voltammetric measurements are given which relate the lowered oxidation potentials of hydrogen-bonded phenols to pyridine basicity and enhanced quenching rates. These data help clarify the circumstances in which both concerted proton movement and solvation play essential roles in the electron-transfer process. Kinetic deuteration effects are demonstrated for these reactions, confirming and extending earlier interpretations. Finally, using previously measured extinction coefficients of C_{60} triplet and radical anion, we obtain radical yields in these reactions which also reflect solvation effects on the detailed quenching mechanism.

Experimental Section

Materials. C_{60} (≥99.94%) was obtained from the SES Research Co. Solvents (Aldrich HPLC grade) were dried over molecular sieves. Phenols and pyridines were recrystallized or distilled. Phenols were deuterated by fast exchange with CH_3OD (D > 99%), added to the solution in 20-fold excess. As used here the terms "phenol" and "pyridine" are generic. Specific compounds are denoted as follows: 3-chloropyridine = 3-Cl-Py; pyridine = Py; collidine = 2,4,6-trimethylpyridine = TMP. Substituted phenols and naphthols are identified as such.

Apparatus and Procedure. 1. Hydrogen-Bonding Equilibria. Formation constants for hydrogen-bonded phenol−pyridine complexes were determined spectroscopically from the accompanying red shift in UV phenol absorption, for comparison with kinetically measured values. For these systems, Mataga et al.[4] have shown that

$$[1 - A_0/A]_\lambda/[\text{base}]_0 = -K + K(\epsilon_C/\epsilon_A)_\lambda(A_0/A) \qquad (1)$$

where A and A_0 are the absorbances of phenol solutions at a particular wavelength, respectively, with and without addition of base, and ϵ_C and ϵ_A are the respective extinction coefficients of complexed and free phenol. Plotting the left-hand function against A_0/A typically gave good lines, with data at different wavelengths converging to a common

[⊗] Abstract published in *Advance ACS Abstracts,* December 15, 1997.

(1) Biczók, L.; Linschitz, H. *J. Phys. Chem.* **1995**, *99*, 1843.

(2) Gupta, N.; Linschitz, H.; Biczók, L. *Fullerene Sci. Technol.* **1997**, *5*, 343.

(3) Babcock, G. T.; Barry, B. A.; Debus, R. J.; Hoganson, C. W.; Atamian, M.; McIntosh, L.; Sithole, I.; Yocum, C. F. *Biochemistry* **1989,** *28,* 9557.

(4) (a) Mataga, N.; Tsuno, S. *Bull. Chem. Soc. Jpn.* **1957**, *30* , 368. (b) Miyasaka, H.; Tabata, A.; Ojima, S.; Ikeda, N.; Mataga, N. *J. Phys. Chem.* **1993**, *97*, 8222.

S0002-7863(97)02752-2 CCC: $14.00

Table 1. Quenching of $^3C_{60}$ by Various Phenol−Pyridine−Solvent Systems: Reaction Parameters

phenol substs	base	solvent	E_p^{ox}, V vs SCE[a]	K, M^{-1}, spect.	K, M^{-1}, kinet.	$-\Delta G_{app}$,[b] eV	k_{QB}, 10^7 M^{-1} s^{-1}
H		PhCN	*c*				<0.1
	TMP	PhCN	1.26		6.7 ± 0.9	−0.07	6.0 ± 0.3
4-Me	−	PhCN	1.54				<0.1
	Cl-Py	PhCN	1.24				
	Py	PhCN	1.06	2.8 ± 0.2	2.6 ± 0.3	0.13	19 ± 1
	TMP	PhCN	0.98	5.5 ± 0.6	6.9 ± 0.9	0.21	53 ± 3
	Py	CH_2Cl_2		16 ± 2	15 ± 3		4.4 ± 0.2
	TMP	CH_2Cl_2		30 ± 2	36 ± 4		32 ± 5
4-MeO	−	PhCN	1.29			−0.10	0.44 ± 0.04
	BQ[d]	PhCN			1.1 ± 0.2		40 ± 4
	ClPy	PhCN	1.04	0.9 ± 0.2	1.1 ± 0.2	0.15	96 ± 8
	Py	PhCN	0.84			0.35	230 ± 20
	TMP	PhCN	0.76	6.0 ± 0.6	4.8 ± 0.5	0.43	250 ± 20
	Py	CCl_4		33 ± 3	*x*		*x*
	TMP	CCl_4		82 ± 5	86 ± 11		160 ± 10
2-MeO	−	PhCN	1.41				<0.1
	Cl-Py	PhCN	1.12	*e*			
	Py	PhCN	0.90	*e*	0.7 ± 0.3	0.29	210 ± 50
	TMP	PhCN	0.84				
	Py	CH_2Cl_2		2.4 ± 0.3	2.1 ± 0.2		67 ± 3
	TMP	CH_2Cl_2		2.4 ± 0.3	2.2 ± 0.2		190 ± 10
	Py	toluene			*x*		*x*
	Py	CCl_4		1.4 ± 0.3	*x*		*x*
	TMP	CCl_4		3.0 ± 0.5	*y*		*y*
2,6-DiMeO	−	PhCN	1.27			−0.08	0.45 ± 0.03
	ClPy	PhCN	0.90	*e*	0.9 ± 0.2	0.29	170 ± 20
	Py	PhCN	0.69	*e*		0.50	250 ± 20
	TMP	PhCN	0.60	*e*		0.59	260 ± 20
	Py	CCl_4		1.5 ± 0.3	*x*		*x*
	TMP	CCl_4		2.0 ± 0.5	3.0 ± 0.5		310 ± 30
3-CN	−	CH_3CN	2.25[f]				
	TMP	PhCN	1.27	12 ± 1		−0.08	0.35 ± 0.05
4-OH	−	PhCN	1.20			−0.01	1.2 ± 0.2
	ClPy	PhCN	0.80		1.2 ± 0.3	0.39	250 ± 20
	Py	PhCN	0.60		3.4 ± 0.3	0.59	330 ± 40
	TMP	PhCN	0.53	6 ± 3	9.5 ± 0.6	0.66	270 ± 10
	TMP	toluene		43 ± 5	36 ± 3		410 ± 20
	TMP	CCl_4		38 ± 3	37 ± 3		270 ± 20
2-OH	−	PhCN	1.20			−0.01	2 ± 0.5
	Pyd[d]	PhCN	0.83		2.7 ± 0.5	0.36	90 ± 10
	Py	PhCN	0.72	3.3 ± 0.2	2.8 ± 0.5	0.42	220 ± 30
2,3,5,6-tetra-Me-4-OH	−	PhCN	0.86	−	−	0.33	220 ± 20[g]
2,3,5-tri-Me-4-OH		PhCN	0.93			0.26	200 ± 30[g]
2,3-di-Me-4-OH		PhCN	1.02			0.07	86 ± 10[g]
2-Me-4-OH		PhCN	1.12			0.07	11 ± 2[g]
1-naphthol[h]	−	PhCN	1.39			−0.20	0.25 ± 0.03
	ClPy	PhCN	0.98		3.3 ± 0.2	0.21	55 ± 5
	Py	PhCN	0.84	5.0 ± 0.5	4.4 ± 0.2	0.35	200 ± 20
	TMP	PhCN	0.76	9.5 ± 0.5	9.4 ± 0.5	0.43	260 ± 30
	−	CH_2Cl_2					<0.2
	Cl-Py	CH_2Cl_2		10 ± 0.5	9.8 ± 0.5		21 ± 5
	Py	CH_2Cl_2		30 ± 2	25 ± 2		300 ± 20
	TMP	CH_2Cl_2		62 ± 2	58 ± 5		450 ± 40
	−	CCl_4					<0.1
	Cl-Py	CCl_4		22 ± 2			<0.1
	Py	CCl_4		82 ± 8	*x*		*x*
	TMP	CCl_4		220 ± 30	170 ± 30		140 ± 40
2-naphthol	−	PhCN					0.6 ± 0.04
	TMP	PhCN		7.5 ± 0.2	7.2 ± 0.3		110 ± 20

[a] These peak potentials of the phenols (without pyridines) agree closely with those obtained by cyclic voltammetry in acetonitrile−0.1 M Et_4NBF_4 or in CH_2Cl_2−0.1 M Et_4NBF_4.[18c] [b] ΔG_{app} = apparent ΔG; calculated from peak potentials using $E_T(C_{60}) = 1.57$ eV[36] and taking charge separation distance = 8 Å. [c] Obscured by the solvent−electrolyte oxidation potential window. [d] BQ = 7,8-benzoquinoline; Pyd = pyridazine. [e] Too small to measure. [f] Reference 18c. [g] Biczok, L.; Linschitz, H.; Treinin, A., *Fullerenes: Recent Advances in the Chemistry and Physics of Fullerenes and Related Materials*; Kadish, K. M., Ruoff, R. S., Eds.; The Electrochemical Society: Pennington, NJ, 1994; pp 909−920. [h] Reference 2. [x] Rate vs base concentration is concave. [y] Rate vs base concentration is linear.

intercept, corresponding to the equilibrium constant, K. The derivation of hydrogen-bonding constants from the kinetic data is described below.

2. Polarographic Measurements. Cyclic voltammograms in benzonitrile solutions were recorded on an EG&G Versastat potentiostat, using a polished glassy carbon working electrode, Pt wire counter electrode, and Ag−AgCl reference electrode, with tetra-*n*-butylammonium hexafluorophosphate ($TBAPF_6$) as the supporting electrolyte and C_{60}, $E(C_{60}/C_{60}^{\bullet-}) = -0.45$ V vs SCE, as an internal reference.[5] All phenol and naphthol oxidations were irreversible, at sweep rates up to 5 V/s. The peak potentials, E_p^{ox}, for the oxidation of phenols in the absence and presence of pyridines are reported in Table 1, column 4. The difference between the peak potentials for C_{60} reduction and phenol oxidation, directly measured in the same solution, were used in the calculations of an *apparent* free enthalpy change, ΔG_{app}.

(5) Dubois, D.; Moninot, G.; Kutner, W.; Jones, M. T.; Kadish, K. M. *J. Phys. Chem.* **1992**, *96*, 7137.

3. Flash Photolysis. Solutions of C_{60} containing appropriate reactants were purged with nitrogen and studied by flash photolysis, using a tunable flashlamp-pumped dye laser (Cynosure, ED-200) providing excitation at 590 nm (Rhodamine 6G) and 0.2 μs fwhm. Flash transients were followed by conventional means,[6] using a photomultiplier to 800 nm and InGaAs photodiode and fast amplifier (New Focus, 1811) for the near-IR, and recorded by a fast 10-bit digitizer (Tektronix RTD710A) and computer. Quenching rate constants were determined from the linear dependence on quencher concentration of the pseudo-first-order decay of $^3C_{60}$ absorption at 750 nm.[7a] Concentrations were adjusted so that the triplet decay was dominated by the pseudo-first-order term. Radical yields were determined from the ratio of initial (triplet) to long-lived (radical) absorbances, corrected for any overlapping decay,[7b] and using extinction coefficients measured previously.[7a,c] Transient absorbances were obtained either from single oscillograms at 500 nm or averaged over successive sweeps at 750 nm (triplet) and 1080 nm ($C_{60}^{\bullet-}$),[7c] corrected for flash energy variations. At the wavelengths used, there is no interfering phenoxy radical absorption.

Results and Discussion

Table 1 summarizes the oxidation potentials, spectroscopic and kinetic hydrogen-bonding equilibrium constants, and quenching rate constants for all phenol−base−solvent systems studied. These were chosen to include as wide a range as possible of phenol oxidation potential and acidity and pyridine basicity within the available range (about 4 orders of magnitude) of measurable quenching rates. For each phenol, the data are arranged in order of decreasing solvent polarity as measured by their $E_T(30)$ values (benzonitrile, 41.5; CH_2Cl_2, 40.7; toluene, 33.9; CCl_4, 32.4 kcal/mol)[8] and within each solvent group, increasing pyridine basicity (pK_a's in acetonitrile: 3-Cl-Py, 9.0; Py, 12.3; TMP, 16.8).[9,10]

1. Spectroscopic Hydrogen-Bonding Equilibrium Constants. Figure 1 illustrates the determination of the hydrogen-bonding equilibrium constants listed in Table 1 for a representative system, 4-methoxyphenol−TMP in CCl_4. The typical red shift of the long-wavelength phenol absorption upon hydrogen bonding[4] and the application of eq 1 to these data are shown in Figure 1, parts A and B, respectively. The formation constants listed in Table 1 agree very closely with previous measurements of the same cases, such as bonding by Py to 4-methoxyphenol[11] and 1-naphthol.[12] As is generally observed, the K's increase with increasing base strength of the pyridines and decrease with increasing solvent polarity[13−16] (see data in Table 1 for 4-methylphenol and 1-naphthol). Particularly interesting in this regard is the solvent effect on the 2-methoxyphenol−Py equilibrium, in which the trend with polarity is reversed: K = 2.4 M^{-1} in CH_2Cl_2 and 1.4 M^{-1} in CCl_4. This may indicate

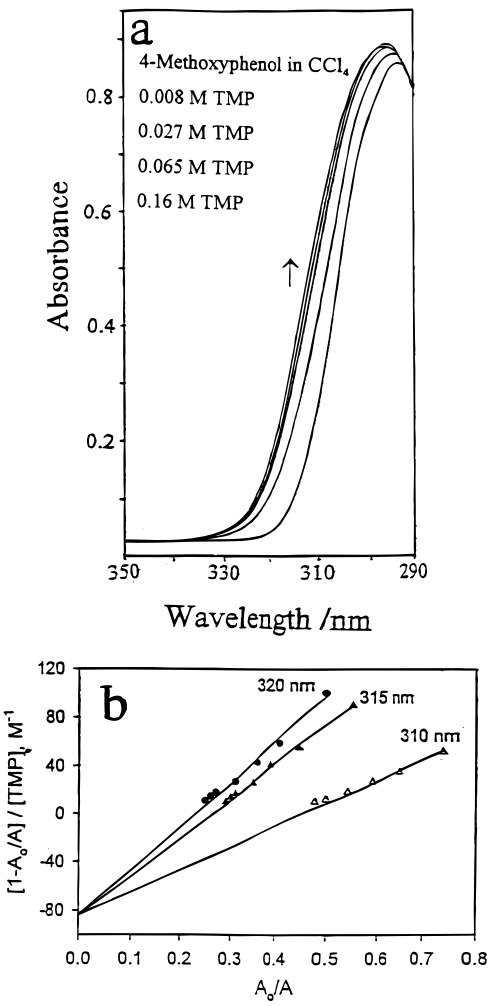

Figure 1. Spectroscopic determination of hydrogen-bonding formation equilibrium constant: 4-MeOPhOH + TMP in CCl_4; (a) change in absorption spectra with added TMP, (b) Mataga plot at three wavelengths.

that competition between intra- and intermolecular H-bonding, in addition to steric hindrance, is involved in hydrogen bonding to this molecule, with low solvent polarity favoring the intramolecular bonding.

2. Polarographic Oxidation of Phenols.[17] In benzonitrile−$TBAPF_6$ solutions, cyclic voltammograms of all the phenols in Table 1 show a single, irreversible two-electron oxidation wave, in agreement with previous observations.[18] In strongly acidified media and at low temperatures, the phenol cation radical is stabilized and reversible one-electron waves are obtained. The irreversibility in neutral medium has therefore been assigned to deprotonation of the phenol cation radical, forming the more easily oxidized phenoxy radical.[18]

Addition of pyridines results in conversion of the original anodic wave to a new, irreversible, prior wave at lower potential (Figure 2A). The shift in potential is largest for TMP (ΔE_p^{ox} = 550−600 mV), less for Py, and least for 3-Cl-Py (~300 mV), corresponding to the decreasing order of basicity (Table 1). The concentration of base needed to complete this change is

(6) Andrews, L. J.; Deroulede, A.; Linschitz, H. *J. Phys. Chem.* **1978**, *82*, 2304.
(7) (a) Biczok, L.; Linschitz, H.; Walter, R. I. *Chem. Phys. Lett.* **1992**, *195*, 339 and references therein. *Ibid*. **1994**, *221*, 188. (b) Andrews, L. J.; Levy, J. M.; Linschitz, H. *J. Photochem.* **1976**, *6*, 355. (c) Steren, C. A.; van Willigen, H.; Biczok, L.; Gupta, N.; Linschitz, H. *J. Phys. Chem.* **1996**, *100*, 8920.
(8) Reichardt, C. *Solvents and Solvent Effects in Organic Chemistry*; VCH: Weinheim, Germany, 1988.
(9) Cauquis, G.; Deronzier, A.; Serre, S.; Vieil, E. *Electroanal. Chem. Interfacial Electrochem.* **1975**, *60*, 205.
(10) Anne, A.; Habiot, P.; Moiroux, J.; Neta, P.; Saveant, J. M. *J. Phys. Chem.* **1991**, *95*, 2370.
(11) Dierckx, A. M.; Huyskens, P.; Zeegers-Huyskens. *J. Chim. Phys.* **1965**, *62*, 336.
(12) Gramstad, T. *Acta Chem. Scand.* **1961**, *16*, 807.
(13) Joesten, M. H.; Schaad, L. J. *Hydrogen Bonding*; Marcel Dekker Inc.: New York, 1974.
(14) Abraham, M. H.; Duce, P. P.; Prior, D. V.; Barrat, D. G.; Morris, J. J.; Taylor, P. J. *J. Chem. Soc., Perkin Trans. 2* **1989**, 1355.
(15) Titov, E. V.; Shurpach, V. I.; Belkina, G. A.; Gonchar, N. P. *J. Mol. Struct.* **1990**, *219*, 257.
(16) Vasin, S. V. *Russ. J. Phys. Chem.* **1985**, *59*,1138.
(17) We give here only a brief summary of essential voltammetric results and interpretations regarding these phenol−additive systems, to relate to their quenching behavior, which is our main concern in this paper.
(18) (a) Hammerich, O.; Parker, V. D.; Ronlan, A. *Acta Chem. Scand. B* **1976**, *30*, 89. (b) Hammerich, O.; Parker, V. D. *Acta Chem. Scand. B* **1982**, *36*, 63 and references therein. (c) Parker, V. D. In *Encyclopedia of Electrochemistry of the Elements*; Bard, A. J., Lund, H., Eds.; Dekker: New York, 1978; Vol. XI. pp 242−275.

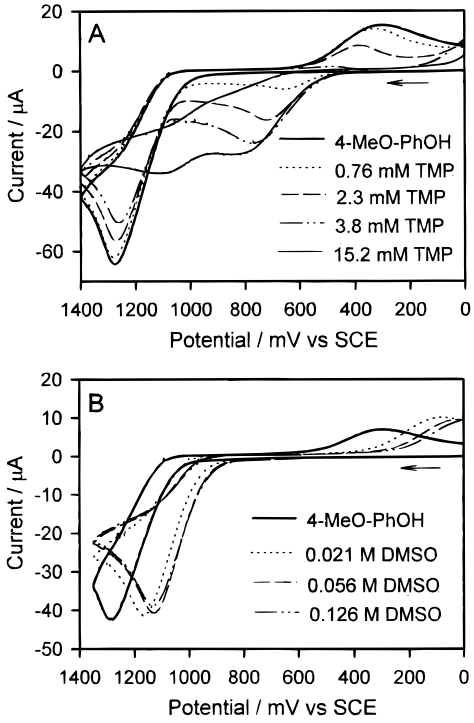

Figure 2. Cyclic voltammograms of 4-MeOPhOH: (A) in the presence of different concentrations of TMP, (B) in the presence of different concentrations of DMSO. Scan rate was 100 mV/s.

comparable to that of the phenol (millimolar) for TMP, somewhat higher for Py, and about 0.1 M for Cl-Py. At intermediate concentrations both the original and new anodic peaks are seen. Peak potentials given in Table 1 thereafter remain constant with added base, up to at least 0.5 M, the range in which the $^3C_{60}$ quenching measurements are done. The new maxima are quite sharply defined for TMP, but broader with Py and more so with Cl-Py. The resulting uncertainty in E_p values of Table 1 is ±0.03 V.

In the rather special case of hydroquinone (QH_2), similar new, irreversible anodic waves at lower potential have also been observed upon addition of 2,6-dimethylpyridine[19] or the stronger base, pyrrolidine,[20] which have been assigned to the oxidation of phenoxide ion: $QH^- \rightarrow Q + H^+ + 2e$.[19−21] While the abrupt appearance of a new anodic wave upon addition of pyridine is consistent with formation of a new species prior to the oxidation process, we rule out phenoxide ion on the following basis: (a) Absorption spectra show that phenoxide is not formed from the phenols, including hydroquinone, even in presence of large excess of the most basic pyridine, TMP, in the polar solvent benzonitrile, but phenols are deprotonated upon addition of stoichiometric amounts of tetra-*n*-butylammonium hydroxide, TBAOH. (b) TBAOH causes much larger changes in potential (∼1 V) than does TMP. A similar large decrease in oxidation potential following addition of TBAOH has also been observed in cyclic voltammograms of 2,4,6-tri-*tert*-butylphenol in acetonitrile.[22] (c) A significant deuterium isotope effect is observed in the pyridine-enhanced quenching reaction (see below).

In sharp contrast to the effects of pyridines, addition of DMSO to the solution leads only to a shift or translation of the original phenol anodic waves to lower potentials. No prior waves appear, even at 1 M DMSO in PhCN or CH_2Cl_2 (Figure 2B).

Table 2. Hydrogen Bonding vs Proton Transfer: Comparative Effects of DMSO and Pyridines

phenol	solvent	base	pK_a[a]	E_p^{ox}	K, M^{-1} [b]	k_{QB}, 10^7 M^{-1} s^{-1}
1-naphthol	CH_2Cl_2	DMSO	−1.54	1.05	30 ± 2	<0.1
	CH_2Cl_2	Py	5.23	0.75	30 ± 2[c]	300
2-MeO−	CH_2Cl_2	DMSO	−1.54	1.21	1.3 ± 0.1	<0.1
	CH_2Cl_2	Py	5.23	0.95	2.4[d]	67
4-MeO−	PhCN	DMSO	−1.54	1.13	6.0 ± 0.5[e]	10
	PhCN	TMP	7.42	0.76	6.0 ± 0.6[f]	250

[a] pK_a of protonated base, in water, from ref 13 and references therein. [b] Values from UV spectroscopy. [c] From kinetics, $K = 25 \pm 2$ M^{-1} (Table 1). [d] From kinetics, $K = 2.1 \pm 0.2$ M^{-1}. [e] From kinetics, $K = 3.5 \pm 0.2$ M^{-1}. [f] From kinetics, $K = 4.8 \pm 0.5$ M^{-1} (Table 1).

The limiting peak potentials of the shifted waves are significantly higher than those of the new waves obtained by treatment with pyridines (Tables 1 and 2).

We attribute the different electrochemical behaviors of the pyridine and DMSO systems in Figure 2 to different rates and ΔG values for proton transfer to the added base, associated with oxidation of hydrogen-bonded phenols.[23] This view is supported by the respective pK_a values for pyridines and DMSO (Table 2), relative to those of the phenol cation radicals. For the latter compounds in Table 2, these pK_a's in DMSO, obtained by Bordwell and Cheng,[24] are 1-naphthol$^+$, −6.7; 2-MeOPhOH$^+$, −6.4; 4-MeOPhOH$^+$, −4.7. Thus ΔpK_a's for the assumed proton transfer are much greater for the pyridines than for DMSO. In addition, the concentration of pyridines required to develop the new anodic peak increases with decreasing pK_a. Further discussion of these voltammograms is given below, in connection with the mechanism of reductive quenching by phenols. In any case, Figure 2A and Table 1 establish a significant lowering of phenol oxidation potentials, directly correlated with the basicity of the added pyridines.

3. Interaction of $^3C_{60}$ with Hydrogen-Bonded Phenols. a. Identification of Reaction Products. The overlap and generally low extinction of the absorption spectra of relevant species other than $^3C_{60}$ and $C_{60}^{\bullet-}$ make it difficult to identify transients in the reaction discussed here. However, these may be resolved following the flash excitation of C_{60} in benzonitrile containing the reducing system 4-methoxyphenol and 7,8-benzoquinoline. The extinction coefficients (M^{-1} cm^{-1}) of neutral 4-methoxyphenoxy radical (403 nm) and protonated 7,8-benzoquinoline (370 nm) are respectively 8200[25] and 14 400,[26] while the absorption of $C_{60}^{\bullet-}$ is relatively low ($\epsilon \approx 4000$) and rather flat throughout this region.[7a,27] Thus the time-resolved spectra of Figure 3A show the conversion of $^3C_{60}$ to $C_{60}^{\bullet-}$ at 1080 nm,[7c] together with formation of neutral phenoxy and protonated benzoquinoline. The assignment of the 370 nm transient is confirmed by the disappearance of this peak, leaving only the phenoxy band (Figure 3A, insert) when benzoquinoline is replaced by TMP, which also leads to reduction of $^3C_{60}$ at the same rate. Thus, the electron and proton are shown to move from the common donor, 4-methoxyphenol to different respective acceptors:

(19) Parker, V. D. *Chem. Commun.* **1969**, 716.
(20) Eggins, B. R. *Chem. Commun.* **1969**, 1267.
(21) Eggins, B. R.; Chambers, J. Q. *J. Electrochem. Soc.* **1970**, *117*, 186.
(22) Richards, J. A.; Whitson, P. E.; Evans, D. H. *J. Electroanal. Chem.* **1975**, *63*, 311.
(23) Gupta, N.; Linschitz, H. *J. Am. Chem. Soc.* **1997**, *119*, 6384, where H-bonding is shown to facilitate reversible quinone reduction.
(24) Bordwell, F. G.; Cheng, J. P. *J. Am. Chem. Soc.* **1991**, *113*, 1736.
(25) (a) Das, P. K.; Encinas, M. V.; Steenken, S.; Scaiano, J. C. *J. Am. Chem. Soc.* **1981**, *103*, 4162 (relative to $\epsilon = 5500$ M^{-1} cm^{-1} for benzophenone ketyl: Inbar, S.; Linschitz, H.; Cohen, S. G. *J. Am. Chem. Soc.* **1981**, *103*, 7232). (b) Johnston, L. J.; Mathivanan, N.; Negri, F.; Siebrand, W.; Zerbetto, F. *Can. J. Chem.* **1993**, *71*, 1655.
(26) Nasielski, J.; Nonckt, E. V. *Spectrochem. Acta* **1963**, *19*, 1989.
(27) Kamat, P. V. *J. Am. Chem. Soc.* **1991**, *113*, 9705.

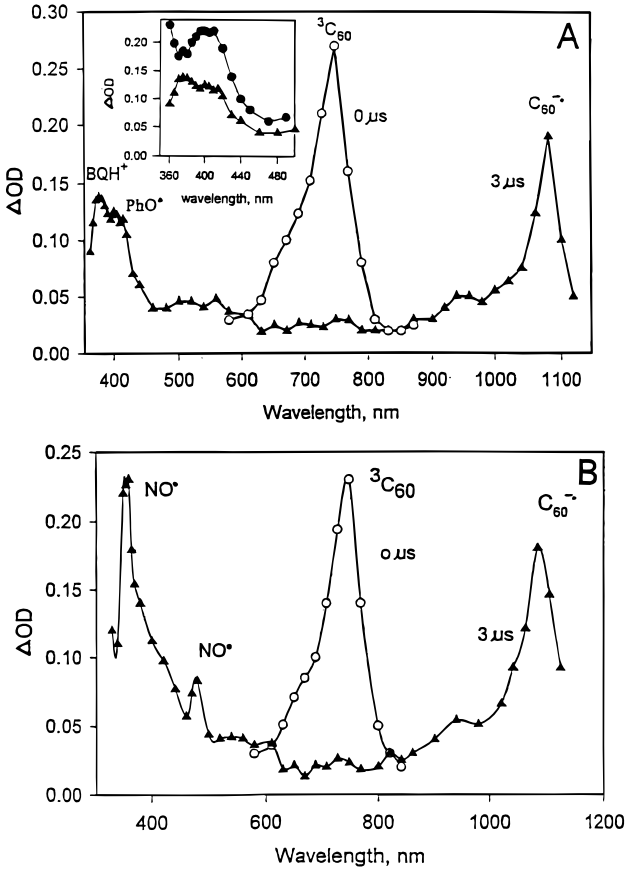

Figure 3. Time-resolved absorption spectra: (A) 0.3 mM C_{60} + 5.0 mM 4-MeOPhOH + 0.5 M 7,8-benzoquinoline in PhCN, immediately (0 μs) and 3 μs after the flash. Insert: comparison of spectra obtained with two different bases: (●) TMP; (▲) 7,8-benzoquinoline (the higher absorbance of the phenoxy radical in the TMP reaction represents higher yield). (B) 0.3 mM C_{60} + 1.5 mM 2-naphthol + 0.5 M TMP in PhCN.

$$^3C_{60} + \text{4-MeOPhOH- - -B} \rightarrow C_{60}^{\bullet-} + \text{4-MeOPhO}^\bullet + BH^+$$

where B is the aza-aryl base.

Additional evidence for this reaction is given in Figure 3B,[28] which shows the formation of the well-characterized spectrum of neutral 2-naphthoxy radical[25] in the TMP-catalyzed reduction of $^3C_{60}$. In this case, absorption of the presumed protonated TMP is obscured. From the ΔOD peaks of Figure 3B, using extinction coefficients of naphthoxy (25 000 M^{-1} cm^{-1})[25] and $C_{60}^{\bullet-}$ (18 600 M^{-1} cm^{-1})[7a,c] radicals and C_{60} ground state, we estimate the relative radical yields $NO^\bullet/C_{60}^{\bullet-} = 1.1 \pm 0.25$. Information on the nature of the transition state is derived from the kinetic studies.

b. Kinetics of Pyridine-Enhanced Quenching. The effect of pyridines on the second-order quenching rate constants of $^3C_{60}$ by phenols is shown for some representative systems in benzonitrile and methylene chloride (Figure 4) and CCl_4 (Figure 5). In these plots, k is the effective, measured pseudo-first-order rate constant for triplet decay in phenol−base solutions, k_0 is the rate constant in the same solution in absence of phenol, and $[PhOH]_o$ is the total phenol concentration. Since the rate increases with increasing pyridine concentration, $[PhOH]_0$ is decreased correspondingly in studying a given system to maintain the triplet lifetime within accurately measurable limits (∼1−2 μs) and in a range in which triplet decay is entirely dominated by the first-order term.

We first discuss the results shown in Figures 4 and 5A, in which the rate constant rises initially with added pyridine and then tends to level off. This *convex* behavior is observed for all systems in the polar solvents, benzonitrile and methylene chloride (Figure 4), but in CCl_4 is seen only in phenol−TMP solutions (Figure 5A).

As before, we attribute these pyridine-enhanced rates to quenching by hydrogen-bonded phenol−base pairs.[1,2] On this assumption, and with the condition that the total concentration

(28) Reprinted from ref 2, p 346, by courtesy of Marcel Dekker, Inc.

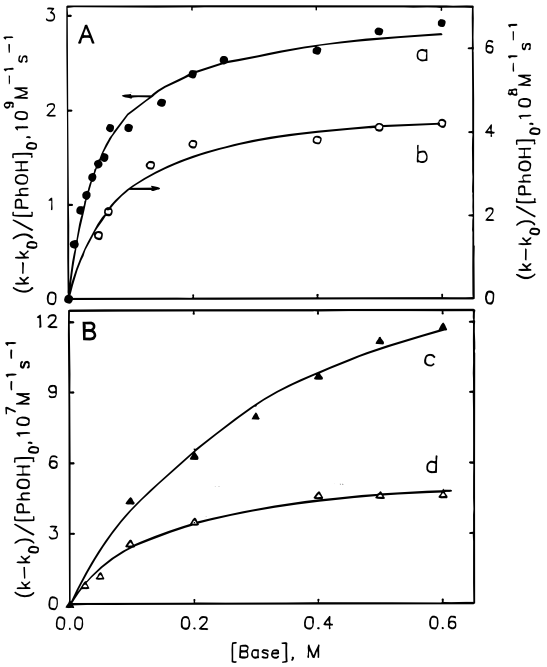

Figure 4. Effect of hydrogen-bonding additives on the rate of quenching of $^3C_{60}$: (a) 1-naphthol + Py in CH_2Cl_2; (b) 4-MeOPhOH + TMP in PhCN; (c) 4-MeOPhOH + Py in CH_2Cl_2; (d) PhOH + TMP in PhCN.

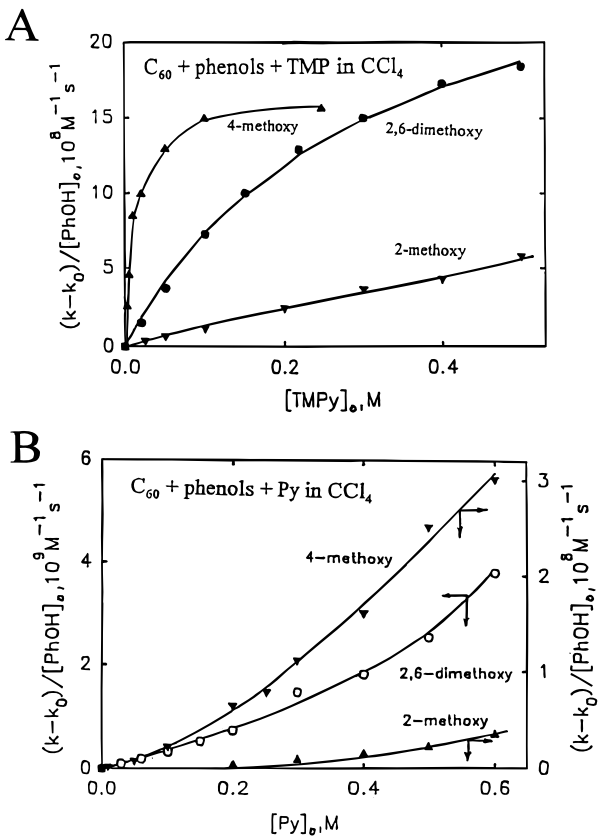

Figure 5. Comparison of the effects of (A) TMP and (B) Py on the rate of quenching of $^3C_{60}$ by different phenols in CCl_4.

of added base, $[B]_0$, much exceeds $[PhOH]_0$, we may write[1]

$$\frac{k - k_0}{[PhOH]_0} = \frac{k_{QB}K[B]_0}{1 + K[B]_0} \quad (2)$$

where k_{QB} and K are respectively the second-order quenching rate and formation equilibrium constants of the hydrogen-bonded phenol−pyridine complex. On the indicated scales, and for the systems shown in Figures 4 and 5, the decay rates, k_0, in absence of phenol or with phenol or pyridine alone[29] are all very small or negligible. The curves of Figures 4 and 5A are nonlinear least-square fits of eq 2 to the experimental points. Table 1 summarizes the resulting best values of K and k_{QB} for these and similar cases in which convex plots are obtained. Comparison of columns 5 and 6 in Table 1 shows that the *kinetically derived values of K agree within experimental uncertainty with the quite independent spectroscopic K's over a very wide range.* For example, in the case of 4-methoxyphenol, this extends from the complex with the weak base, 3-Cl-Py, in polar PhCN ($K \sim 1.0\ M^{-1}$) to that with the strong base, TMP, in nonpolar CCl_4 ($K = 84\ M^{-1}$). This agreement, seen throughout Table 1, further validates our previous identification of the quenching species as the hydrogen-bonded phenol−pyridine pair. However, it is also seen in Table 1 that the values of K are not generally correlated with those of k_{QB}. The more important factors are the decrease in E_p^{ox} of the phenols, which is correlated with the basicity of the pyridines (as measured by their pK_a's) and the solvent polarity. Thus the quenching rate for a given phenol can be systematically controlled, up to the diffusion limit, by varying either or both of these factors. In PhCN, the strongest reductant, tetramethylhydroquinone, quenches triplet C_{60} at close to diffusion-controlled rate without base assistance, while the weakest, 3-cyanophenol, despite a rather high value of K, quenches at a barely measurable rate, limited by the k_0 term, even in presence of TMP.

As indicated, the pyridines function in these reactions essentially as proton acceptors rather than simply as hydrogen-bonding agents. This is further demonstrated by the results of quenching by phenols using DMSO or triethyl phosphate as basic additives. Both these compounds are strong hydrogen-bonding agents[13,14] but weak proton acceptors[13,14,30] and cause little or no enhancement of the quenching rate. Table 2 compares the kinetic parameters for DMSO and pyridines, including pK_a's, hydrogen-bonding equilibrium constants, K, and quenching rate constants, k_{QB}. Limiting values of k_{QB} less than $10^6\ M^{-1}\ s^{-1}$ for DMSO were derived from triplet decay measurements at DMSO concentrations up to 1.0 M, and the base−solvent systems in Table 2 are those for which spectroscopically determined K's closely match those of the pyridines. It is evident that, despite similar hydrogen-bonding interactions with the phenols, DMSO does not function as do the pyridines to enhance $^3C_{60}$ quenching. The case of 4-methoxyphenol, for which DMSO does show some positive quenching effect, corresponds also to the most easily oxidized phenol in Table 2, and even here, the deuterium isotope effect is much smaller than that for the pyridines (see below). Generally similar results were obtained with triethyl phosphate.

The combined effects of base strength and solvent polarity are particularly manifest in the different responses of methoxy-substituted phenols in CCl_4, toward addition of TMP and Py (Figure 5A,B). The increase in quenching rate of 4-methoxy- and 2,6-dimethoxyphenol with added TMP (Figure 5A) resembles the curves of Figure 4 and also fits eq 2. The least-squares-derived equilibrium constants, K, match the spectroscopic values and the k_{QB}'s are in the $10^9\ M^{-1}\ s^{-1}$ range (Table 1). However, with the weaker base, Py, the form of the functions (Figure 5B) which rise slowly with continuously increasing slope, is quite different from the convex curve found for the same phenols with TMP. These *concave* functions (Figure 5B) whose occurrence is indicated by *x* in Table 1, clearly cannot correspond to eq 2. Moreover, this effect cannot be ascribed to a lower hydrogen-bonding constant toward the weaker base, since K (spectroscopic) for 4-methoxyphenol−Py in CCl_4 has a quite high value, $33\ M^{-1}$. Thus the system is mostly hydrogen-bonded at Py concentrations as low as 0.1 M, where the quenching rate is just beginning to rise (Figure 5B). Similarly, for 2,6-dimethoxyphenol, the K value for Py complexation ($1.5 \pm 0.3\ M^{-1}$) is not much less than for TMP ($2.0 \pm 0.5\ M^{-1}$), while the functional response to added base is quite different. Direct quenching by Py itself, independently of the hydrogen-bonded complex, is ruled out by the blank experiment. The essential difference between the two bases thus lies in the larger k_{QB} values, correlated with more favorable values of E_p^{ox}, of TMP−phenol pairs.

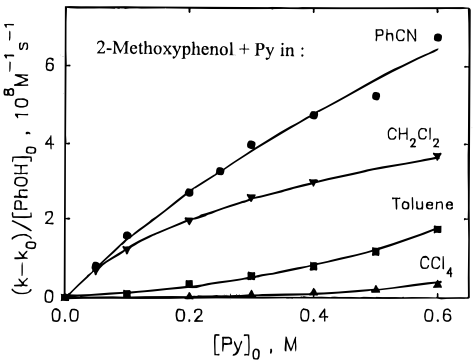

Figure 6. Effect of solvent polarity on the rate of reductive quenching of triplet C_{60} by 2-MeOPhOH−Py system.

We therefore attribute the behavior shown in Figure 5B to nonspecific solvation of the weakly quenching phenol−pyridine pairs by the excess of polar additive, Py. The low Py concentration range (<1 M) at which the rate constant rises indicates further that the solvation is not a simple mole fraction contribution to the local polarity, but is preferential, involving considerable solvent segregation. Such an effect is found, for example, in the decay of triplet 9,10-anthraquinone-2-sulphonate in H_2O-CH_3CN mixtures.[31] The resulting rate enhancement is in accord with well-known solvent polarity effects on electron-transfer quenching in numerous systems, particularly when the driving force of the reaction is small. In this connection, with specific regard to $^3C_{60}$, we have previously found similar polarity dependence in reductive quenching by tritolylamine in benzonitrile, toluene, and CCl_4, for which the rate constants ($M^{-1}\ s^{-1}$) are respectively 3.5×10^9, 8.5×10^7, and $\sim 2 \times 10^6$.[7a]

This interpretation is supported by the solvent-dependent behavior of 2-methoxyphenol, whose quenching rate is least responsive (Figure 5B) to Py addition in CCl_4. Figure 6 shows the effect of Py on the rate constant in different solvents. In CCl_4 and toluene, whose $E_T(30)$ polarity indices are respectively 32.4 and 33.9 kcal/mol, and much lower than that of Py (40.5), the dependence of rate on pyridine concentration is the concave function of Figure 5B. However, in more polar media, CH_2Cl_2 (40.7) and PhCN (41.5), in which the role of preferential solvation should be minimized, the effect of Py approaches that of TMP. The rate vs base function becomes increasingly convex

(29) Arbogast, J. W.; Foote, C. S.; Kao, M. *J. Am. Chem. Soc.* **1992**, *114*, 2277.

(30) Arnett, E. M.; Mitchell, E. J. *J. Am. Chem. Soc.* **1971**, *93*, 4052.

(31) Loeff, I.; Treinin, A.; Linschitz, H. *J. Phys. Chem.* **1983**, *87*, 2536.

Table 3. Radical Yields in Quenching of $^3C_{60}$ by 1-Naphthol and 2-Methoxyphenol: Effects of Base and Solvent

solvent	base	[base], M	ϕ_R
		1-Naphthol[a]	
CCl_4	TMP	0.03	0.02 ± 0.01
		0.30	0.18 ± 0.02
PhCN	TMP	0.05	0.85 ± 0.03
		0.50	0.80 ± 0.03
		2-Methoxyphenol	
CCl_4	TMP	0.05	<0.02
		0.1	0.02 ± 0.01
		0.2	0.05 ± 0.02
		0.5	0.09 ± 0.03
		0.7	0.14 ± 0.03
CCl_4	Py	0.3	0.15 ± 0.03
		0.7	0.21 ± 0.03
CH_2Cl_2	TMP	0.15	0.23 ± 0.03
		0.25	0.24 ± 0.02
		0.50	0.26 ± 0.03
CH_2Cl_2	Py	0.20	0.46 ± 0.03
		0.40	0.48 ± 0.03
PhCN	Py	0.05	0.47 ± 0.03
		0.5	0.42 ± 0.03

[a] Reference 2.

while the specific role of hydrogen bonding is again evidenced by the agreement of the kinetic and spectroscopic hydrogen-bonding equilibrium constants (albeit with considerable uncertainty due to small values of *K*; Table 1). Moreover, the rate constants derived from eq 2 are significantly higher in PhCN (2.1×10^9 M^{-1} s^{-1}) than in the less polar CH_2Cl_2 (6.7×10^8 M^{-1} s^{-1}). The respective contribution of base strength and polarity to the quenching rate becomes, of course, more difficult to resolve as it approaches diffusion control. Of particular interest is the 2-methoxyphenol−TMP−CCl_4 system, for which the almost linear character of its curve in Figure 5A (*y*, in Table 1), falling between concave and convex behavior, indicates that both factors are involved more or less to the same extent.

The pyridazine−catechol (1,2-diazabenzene and 1,2-dihydroxybenzene) pair was examined, with the possibility in mind that a doubly hydrogen-bonded complex might be formed, with interesting values of *K* and k_{QB}. However, in benzonitrile, this complex has a rather low *K*, comparable to that of pyridine[14] and behaves kinetically about in accord with its E_p^{ox} value in Table 1.

4. Quantum Yields and Solvation. Table 3 lists values of bulk quantum yields of C_{60} anion radical in the quenching of $^3C_{60}$ by 1-naphthol and 2-methoxyphenol in various solvent−base systems. Quencher concentrations are adjusted so that yields are given at 95% trapping of the triplet, as measured by transient lifetimes. With 1-naphthol, interactions in all base−solvent systems except Py−CCl_4 follow convex rate vs base concentration functions,[2] while for 2-methoxyphenol and Py, we have seen a shift from concave to convex behavior as solvent polarity is increased from CCl_4 to PhCN (Figure 6). Data for both quenchers show increasing yields with increasing solvent polarity, as usual for reactions forming charged products. For 1-naphthol with TMP, the yield in PhCN is quite high (∼0.8) and independent of base concentration, while in nonpolar CCl_4, Φ_R is much smaller and, in addition, increases with base concentration. The results with 2-methoxyphenol similarly demonstrate these factors. In this case, we find increasing yields with pyridine concentration for both TMP−CCl_4 and Py−CCl_4 systems (Table 3). Moreover, addition of a non-hydrogen-bonding but polar compound, 0.5 M CH_3CN, to 0.1 M Py in CCl_4 raises the radical yield from 0.1 to 0.34 and doubles the quenching rate constant (∼3×10^7 M^{-1} s^{-1}). These findings further support the proposal given above, of a segregated, local

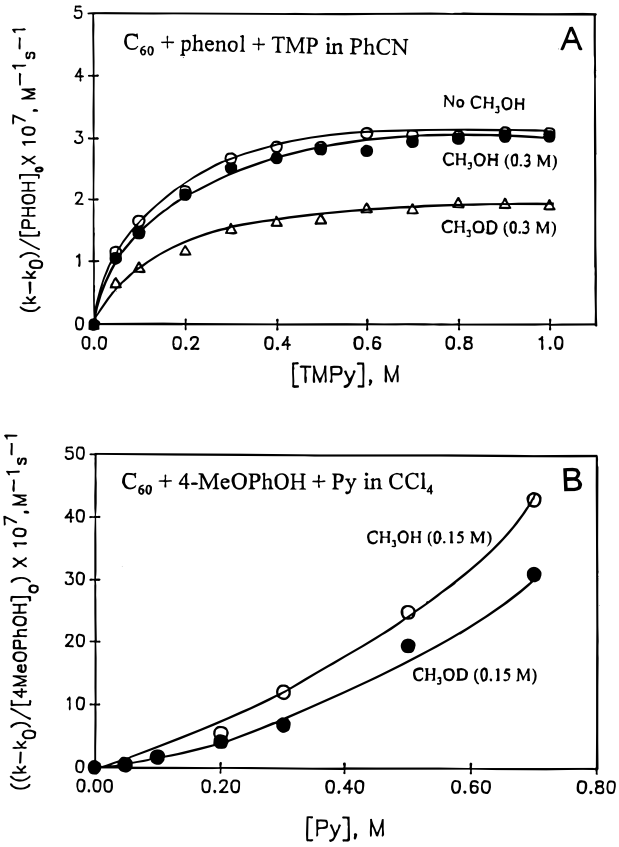

Figure 7. Deuterium isotope effect in reduction of triplet C_{60} by phenol−pyridine systems: (A) PhOH + TMP in PhCN, (B) 4-MeOPhOH + Py in CCl_4.

polar environment or cluster around the reaction complex,[32] to account for the concave curves of Figures 5B and 6. It is noteworthy that, in CH_2Cl_2, 2-methoxyphenol gives higher yields with more polar Py ($\Phi_R = 0.45$) than with TMP ($\Phi_R = 0.25$), although the quenching rates, respectively 6.7×10^8 and 1.9×10^9 M^{-1} s^{-1} (Table 1), are in the reverse order. It appears that, with respect to product separation, the local environment which controls the back-reaction is more important than the relative proton transfer energies which influence the rate.

The detailed nature of the back-reaction raises interesting questions. Within the initial caged reaction complex, electron and proton back-reactions may occur in either a concerted or sequential fashion. However, the back-transfer of the electron from $C_{60}^{\bullet -}$ to the neutral phenoxy radical is itself spontaneous, without involving any proton movement. Oxidation potentials vs SCE of phenoxide ions in PhCN in presence of TBAOH were in the range from −0.3 for hydroquinone to +0.3 V for phenol (see also, ref 22), while the reduction potential of C_{60} is −0.45 V vs SCE.[5] These values make the bulk back-reactions highly favorable. Back reactions followed second-order kinetics and were close to diffusion controlled.[7a]

5. Deuteration and Temperature Effects. Figure 7A,B shows deuteration effects on the rate vs base concentration curves for two systems, with rates well below diffusion control and which respectively display convex (Figure 7A) and concave (Figure 7B) behaviors. Significant isotope effects appear for *both* cases: $k_H/k_D = r = 1.65 \pm 0.1$ for phenol−TMP−PhCN (Figure 7A) and ∼1.37 ± 0.15 for 4-methoxyphenol−Py−CCl_4 at [Py] = 0.7 M (Figure 7B). According to our previous view, we must regard this latter result as only qualitatively significant, since we consider that the solvation shell is changing with

(32) Steadman, J.; Syage, J. A. *J. Am. Chem. Soc.* **1991**, *113*, 6786.

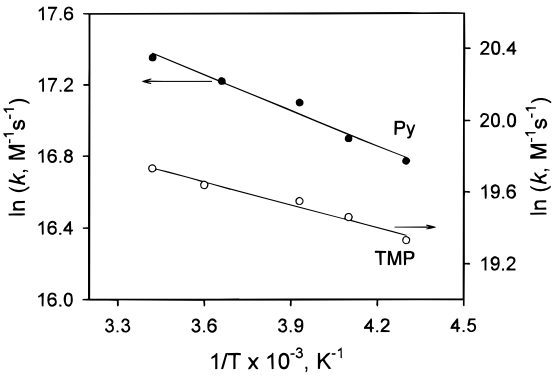

Figure 8. Temperature dependence of pseudo-first-order rate constant for quenching of triplet C_{60} by 4-MePhOH, in PhCN in presence of Py (0.5 M) and TMP (0.3 M).

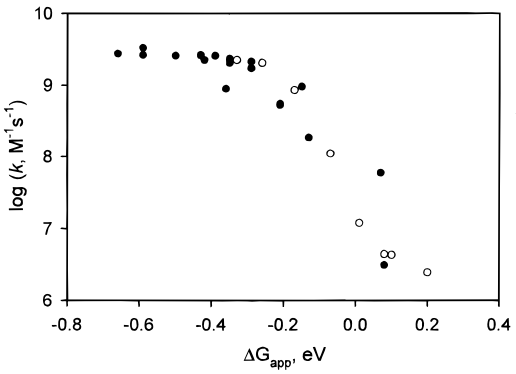

Figure 9. Plot of ΔG_{app} vs log k for quenching of triplet C_{60} by phenols or phenol−pyridine pairs in benzonitrile. Data from Table 1: open circles, without pyridine; filled circles, with pyridine.

increasing [Py] in this solvent. Nevertheless, these results indicate that quenching involves similar transition states for both cases. Moreover, as noted above, the existence of an appreciable kinetic deuterium effect, which evidently requires the phenolic proton, provides further evidence against assignment of pyridine enhanced quenching to a phenoxide species. Measurements on other convex quenching systems all gave r ratios of >1. For *p*-cresol−Py−CH_2Cl_2, with $k_{QB} = 4.4 \times 10^7$ M^{-1} s^{-1}, we obtain $r = 1.5 \pm 0.1$. Even for rates approaching diffusion control, as in 4-methoxyphenol−Py−CH_2Cl_2 ($k_{QB} = 1.8 \times 10^9$ M^{-1} s^{-1}), $r = 1.2 \pm 0.1$.

The isotope effect with the weak protonating agent, DMSO, is much smaller than that with the pyridines. For the system 4-methoxyphenol−DMSO−PhCN, with $k_{QB}(H) = 6.6 \times 10^7$ M^{-1} s^{-1} at 0.5 M DMSO, $r = 1.06 \pm 0.05$.

A few exploratory experiments were also made over a range of temperature. For the systems 4-MePhOH and 4-MePhOD, with Py in CH_2Cl_2, we find that $E_a = 1.26 \pm 0.1$ and 1.41 ± 0.1 kcal/mol, respectively; the small difference associated with deuteration is slightly beyond experimental uncertainty. An effect of pyridine basicity on E_a is also observed; for *p*-cresol−base−CH_2Cl_2, E_a is 1.45 ± 0.2 kcal/mol with Py and 1.0 ± 0.1 kcal/mol with TMP (Figure 8).

6. Relation of Quenching Rates to Oxidation Potentials. We have noted above that the irreversible two-electron anodic waves of phenols correspond to fast proton loss from the oxidized phenol followed by further oxidation of unstable radical products.[18] The onset of a new anodic wave at lower potential and the increase in quenching rate, both correlated with the pK_a of added pyridines, are clearly consistent with the initial step in the electrochemical oxidation mechanism. In this regard, it is significant that much higher concentrations of pyridines are needed to increase the quenching rates of phenols than to lower their voltammetric oxidation potentials. For example, as stated above, addition of TMP in millimolar amounts to benzonitrile solutions of phenols causes immediate appearance of the new anodic wave, and the change is complete at stoichiometric TMP/phenol ratios. However, the quenching rate effects shown in Figures 4−7 are manifested only at hundred-fold higher (>0.1 M) pyridine concentrations, and the rate constants, k_{QB}, listed in Table 1 correspond to the extrapolated plateau values. This difference between the electrochemical and photochemical effects can be understood in terms of the different time scales of the two phenomena[33] and also helps in some degree to clarify the mechanisms of both the electrochemical and photochemical oxidation processes. We have suggested that the new anodic waves seen at low pyridine concentrations represent oxidation of hydrogen-bonded phenols closely coupled to very fast proton transfer to the immediately accessible base. Although absorption spectra may show no bonding at millimolar additive levels, these waves may appear as *kinetic currents*[34] on the slow time scale of voltammetric measurements.[35] By contrast, pyridine-enhanced quenching of $^3C_{60}$ involves a fast electron jump from a necessarily *preformed* hydrogen-bonded phenol−pyridine complex to the triplet (as established experimentally) and a concerted proton movement to the pyridine (as indicated by the deuterium isotope effect). Thus the primary electrochemical oxidation reaction at the lowered potential at low pyridine concentration, although irreversible, may correspond closely to the quenching process at much higher concentrations. However, a concerted proton transfer may not be available to assist quenching by phenols hydrogen-bonded to weakly basic DMSO. These interpretations of the quenching dynamics are supported by the significantly larger kinetic isotope effect for quenching with pyridines compared to quenching with DMSO. On this basis, we might seek a quantitative correlation between the pyridine-enhanced quenching rates and the lowered irreversible oxidation potentials. We note that the detailed interpretation of the potential shift requires not only the pK_a of the added pyridine but also that of the unspecified proton acceptor (impurity, solvent?) in the original solution. Assuming that these potentials leading to the "apparent" free enthalpy values (ΔG_{app}) in Table 1 include the contributions of proton transfer, it is of interest to compare the relation between these values of ΔG_{app} and the rate constants for phenol quenching for the respective cases of absence and presence of pyridine. Since the quenching process involves fast electron transfer coupled with proton movement, one might find in these two situations effects not only arising from differences in oxidation potentials but also attributable to different reorganization energies associated with various proton−acceptor configurations. The available data for the quenching in PhCN solution are plotted in Figure 9. Here,

(33) Peover M. E.; Davis, J. D. *Trans. Faraday Soc.* **1964**, *60*, 476.

(34) (a) Maivanorskii, S. G. *Catalytic and Kinetic Currents in Polarogarphy*; Plenum: New York, 1968. (b) Galus, G. *Fundamentals of Electrochemical Analysis*; Ellis Harwood: Chichester, U.K., 1976; Chapter 8.

(35) We rule out phenoxide oxidation by this same kinetic process on the basis of the relatively small potential shift compared with that caused by TBAOH (see above).

(36) Zeng, Y.; Biczók, L.; Linschitz, H. *J. Phys. Chem.* **1992**, *96*, 5237.

(37) To conveniently distinguish three possible types of closely coupled electron−proton transfer, we suggest the term *concerted* for the case in which both particles move together from a common donor to the same acceptor, *discerted*, in which there is a common donor but different acceptors, and *ascerted*, for different donors to a common acceptor. The examples dealt with here represents discerted transfer. For situations in which motion of the electron and proton can clearly be shown to be sequential, we may replace *...certed* by *...sequent*. Electron transfer via a hydrogen-bond bridge, in which we have proton displacement but not transfer, represents yet another situation.

results on easily oxidized hydroquinones supplement those on phenols, to obtain measurable quenching rates in pyridine-free solutions. However, within the spread of the data, no clear-cut difference between the behavior in presence or absence of pyridine is discernible thus far. Much further work will be needed to distinguish more clearly the overlapping effects of hydrogen bonding, base strength, solvent polarity, and redox potential on these prototype systems.

Summary. The several related findings in this study are summarized as follows:

1. Pyridines greatly enhance the quenching of $^3C_{60}$ by phenols and also lower their oxidation potentials in aprotic solvents.

2. The products of the quenching reaction are identified by flash photolysis as $C_{60}^{\bullet -}$ anion radical, neutral phenoxy (or naphthoxy) radicals, and protonated pyridine.

3. Equilibrium constants for formation of hydrogen-bonded phenol−pyridine pairs, determined by spectrophotometric titrations, agree with those derived from the dependence of second-order quenching rates on pyridine concentration, over a wide range of phenols, pyridines, and solvents.

4. Rate enhancement by added hydrogen-bonding agents correlates with their pK_a's, not hydrogen-bonding power.

5. In a given pyridine−solvent system, k_H/k_D ratios are significantly greater than 1. With DMSO as added base, the isotope effect is essentially nil.

6. Quenching rates increase with solvent polarity. In nonpolar media, convex or concave rate vs pyridine concentration curves are associated respectively with strongly or weakly basic pyridines.

7. Dependence of radical yields on solvent polarity and pyridine concentration parallel the dependence of quenching rates on these parameters.

Conclusions. On the basis of the above results, we conclude the following:

1. The quenching agent in these reactions is the hydrogen-bonded phenol−pyridine pair; the reaction itself involves electron transfer from the phenol to $^3C_{60}$, concerted with proton transfer of the bonding proton to the associated pyridine.[37]

2. The proton transfer contributes to ΔG of the excited state reaction, as indicated directly by the pyridine-induced shift in oxidation potential.

Acknowledgment. We much appreciate the support of this work by the Division of Chemical Sciences, Office of Basic Energy Science, U.S. Department of Energy (Grant FG02-89ER14072) to Brandeis University and by the Hungarian Science Foundation (OTKA, Grant T023428) to L.B. We thank the Soros Foundation for a Travel Grant to L.B.

JA9727528